

# Thermalization of sputtered aluminium atoms in electron cyclotron resonance plasma source

N P Poluektov, V N Kharchenko and I A Kamyschov

Department of Physics, Faculty of Electronics, Moscow State University of Forestry,  
141005 Mytischki-5, Moscow Region, Russia

E-mail: poluekt@mgul.ac.ru

Received 18 October 2002, in final form 14 April 2003

Published

Online at [stacks.iop.org/PSST/12](http://stacks.iop.org/PSST/12)

## Abstract

The transverse temperature of sputtered aluminium atoms in an electron cyclotron resonance discharge has been calculated from the shapes of their Doppler broadening emission lines, which were measured with a pressure scanning Fabry–Perot interferometer. This temperature decreases from 0.8 to 0.28 eV at a distance of 15 cm from the Al target when krypton pressure rises from 0.4 to 4 mTorr. For discharge in argon aluminium temperature falls from 0.5 to 0.18 eV for the same condition.

## 1. Introduction

The ionized physical vapour deposition (IPVD) method is used to deposit materials into high-aspect ratio integrated circuit features such as vias and trenches [1–3]. Sputtering produces a flux of predominately neutral atoms. Anisotropic deposition by IPVD involves ionizing neutral atoms and collimating the ions by accelerating through a plasma sheath. The sputtered atoms are rather energetic—average energy up to 10 eV. The probability of ionization of the sputtered atoms is proportional to their residence time in the region between the target and the sample. This time increases when velocity of sputtered atoms decreases due to collisions with the buffer gas. The subsequent thermalization of the metal atom increases the ionized flux fraction.

The thermalization of sputtered atoms has been investigated theoretically [4–6] using a number of simplifying assumptions and approximations but there is a lack of experimental studies of this problem [7, 8]. In particular, it is difficult to take into account the rarefaction effect of the background gas. The collisions of the energetic metal atoms lead to an increase in the temperature of the inert gas and the density decrease occurs within the region of thermalization [9]. In this paper, we measured the transverse temperature of sputtered aluminium atoms in an electron cyclotron resonance (ECR) plasma source as a function of pressure.

## 2. Experimental apparatus

The experiments were performed in a microwave ECR plasma source. A schematic of the experimental set-up is shown in figure 1. Its detailed description is given in [10]. The vacuum chamber consists of a plasma source (15 cm in diameter and 25 cm long) and a reactor (35 cm diameter and 60 cm long). Microwave power for plasma production up to  $W = 1000$  W (at 2.45 GHz) was introduced into the source via a rectangular waveguide  $90 \times 45$  mm<sup>2</sup> through a quartz window of 2 cm thickness and 15 cm in diameter. The chamber was evacuated

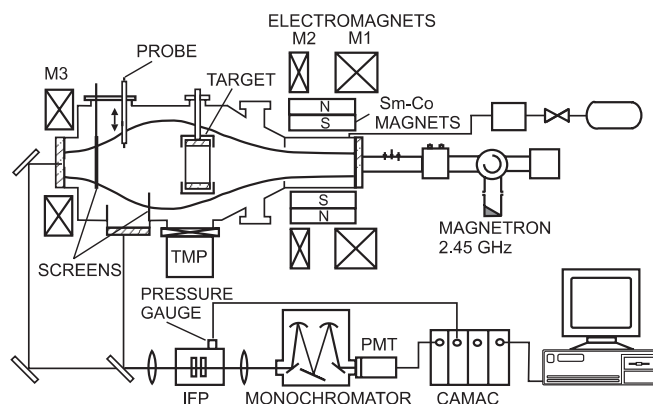


Figure 1. Experimental apparatus.

by turbomolecular pump to base pressure  $10^{-6}$  Torr. The gas pressure  $P$  was measured with the ionization gauge. The working gas injected into the source through a mass flow controller located near the microwave window.

The magnetic field was produced by three electromagnets and 12 permanent Sm–Co magnets. These 12 permanent magnets,  $15 \times 20 \times 120 \text{ mm}^3$  in size with alternative poles, are positioned around the source. They create a cusp magnetic field of 875 G at a distance of 1 cm from the wall. A hollow 5 cm long aluminium cylinder with an inner diameter of 8 cm served as the target. The target was located at  $z = 40 \text{ cm}$  from the entrance quartz window. Such a position of the target prevented the deposition of the metal film on the microwave window and maintained stable discharge during several hours. Negative voltage on the target was 500 V. A third electromagnet M3 located behind the processing chamber resulted in great increase of ion current density downstream. Plasma density up to  $5 \times 10^{11} \text{ cm}^{-3}$  was attained in Kr discharges at pressure 3 mTorr and net power 850 W at this place.

The spatial distributions of ion density, floating and plasma potentials, temperature  $T_e$  and energy distribution function of electrons, measured by a probe are presented in [11]. Measurements in this study were carried out in krypton and argon plasmas at an electromagnetic current of 210 A, which corresponded to a magnetic field of 960 G W near the quartz window. The microwave power  $W_\mu$  was in the range of 500–850 W, reflected power was below 10% of the incident power. Spectra of plasma emission were measured with a grating monochromator (1200 lines  $\text{mm}^{-1}$ , dispersion  $2.4 \text{ nm mm}^{-1}$ ). The random and directed energies of sputtered aluminium atoms were found from spectroscopic measurements using a pressure scanned Fabry–Perot interferometer (IFP) (figure 1).

Plasma emission was monitored through two windows located perpendicular to the flow at  $D = 17.5 \text{ cm}$  downstream from the centre of the target, and parallel to a flow at the end of the reactor. The region of the discharge from which light was collected transverse to the flow was a truncated cone defined by the lens, the aperture in its focal plane and the aperture of the interferometer. The cone increased in diameter from 20 to 25 mm through the discharge.

The pressure scanned IFP was used with a 5–7 mm spacing and had a finesse of 17. The centre of the interference pattern was focused by the lens ( $f = 300 \text{ mm}$ ) on a 0.7 mm pinhole over the entrance slit of a 30 cm monochromator equipped with a photomultiplier tube (PMT). The current output of the PMT was converted to a voltage signal using a direct current amplifier. An RC integrator smoothed off the signal noises. IFP pressure was measured with a strain-gauge transducer. The output signals from the PMT and transducer were fed in two analog-to-digital CAMAC converters.

### 3. Results and discussion

Plasma emission spectrum at 17.5 cm from the target is shown in figure 2. The ratio between the intensities of the ion Al<sup>+</sup> 390.1 nm and atom Al 396.1 nm lines (inset figure) is equal to 0.07, which indicates a high level of aluminium ionization.

At first, we have determined temperature of krypton atoms ( $\lambda = 431.9 \text{ nm}$ ) and ions ( $\lambda = 473.9 \text{ nm}$  and  $476.6 \text{ nm}$ ).

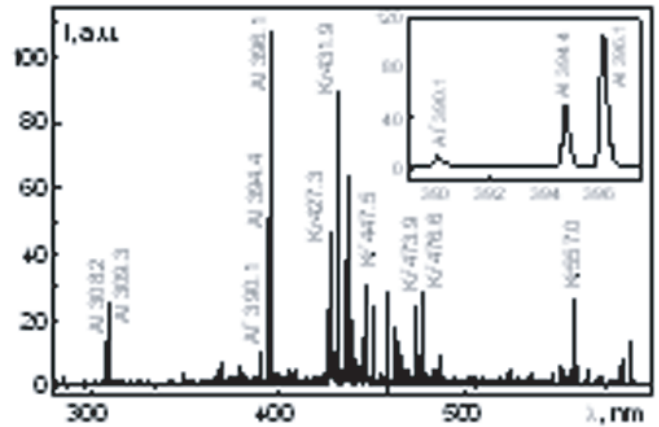


**Figure 2.** Optical emission spectrum at  $D = 17.5 \text{ cm}$ . Kr,  $P = 0.8 \text{ mTorr}$ , flow rate = 10 sccm,  $W_\mu = 850 \text{ W}$ ,  $W_{\text{targ}} = 340 \text{ W}$ .

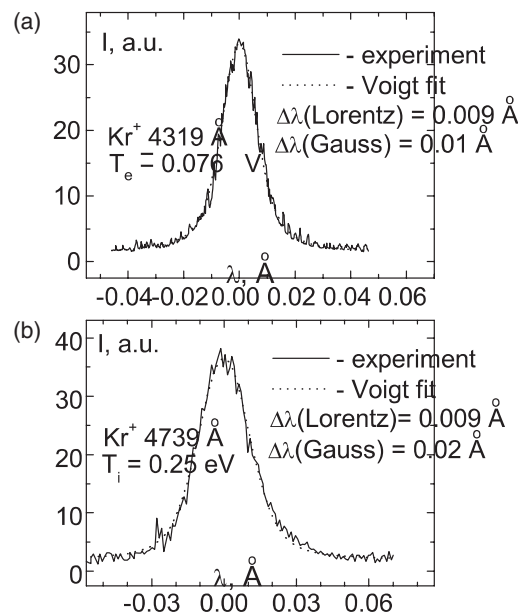


**Figure 3.** The line profiles of Kr 4319 Å (a) and of ions Kr<sup>+</sup> 4739 Å (b), measured in a direction transverse to the flow.  $P = 0.8 \text{ mTorr}$ , flow rate = 10 sccm,  $W_\mu = 800 \text{ W}$ .

Figures 3(a) and (b) show the spectral line profiles of atom (Kr 4319 Å) and ion (Kr<sup>+</sup> 4739 Å), respectively, measured in a transverse direction to the flow. The magnetic field in this region is less than 150 G. The Zeemann broadening is about  $0.001 \text{ Å}$  and its contribution to the line width can be neglected. The instrument broadening was measured by means of a Cd laser. This profile was well fitted by the Lorentzian function with FWHM of  $0.009 \text{ Å}$ . The Fabry–Perot mirrors spacing is 7 mm in this case. The Doppler effect makes the main contribution to the broadening of spectral profile. The experimental contour is well fitted by the Voigt function, which is a Gaussian shape convolved with a Lorentzian one [12]. The reduction procedure allowed us to determine the Gaussian component and calculate from it the temperature. These temperatures were less than 0.1 eV and 0.25 eV, respectively, for 0.8 mTorr, and decreased when pressure rose. These temperatures of atoms and ions are similar to values obtained by laser-induced fluorescence [13, 14] and by optical emission spectroscopy [15]. The ion heating results from the conversion

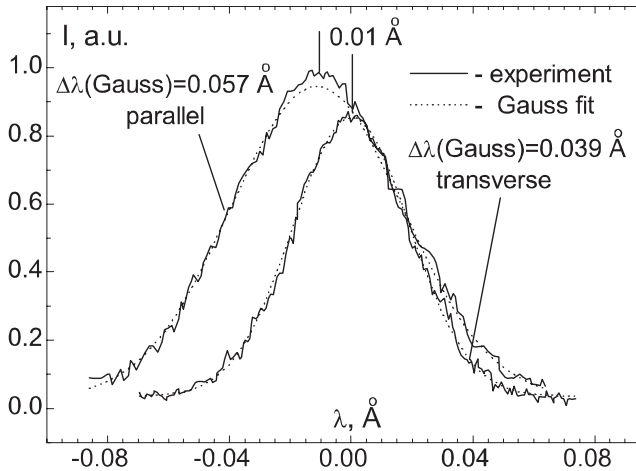


**Figure 4.** The line profiles of Al 3901 Å, measured parallel and perpendicular to the flow directions.  $P = 2.5$  mTorr, flow rate = 25 sccm,  $W_\mu = 600$  W,  $W_{\text{targ}} = 240$  W.

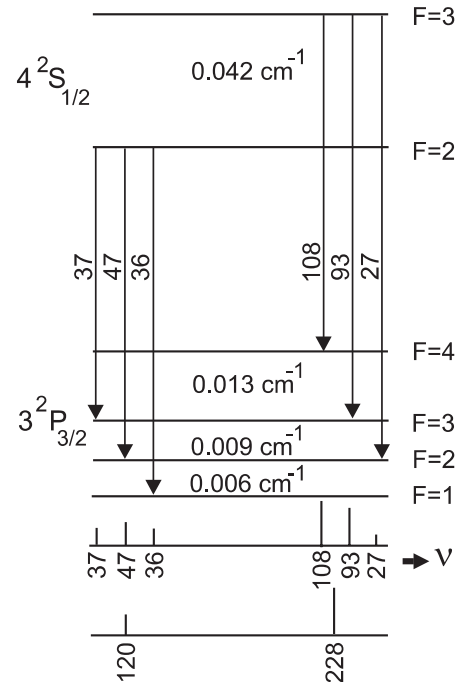
of ion directed energy to random energy through collisions. Ions are accelerated by ambipolar electric field, which depends on both plasma density gradients and electron temperature. The probe measurements of plasma potential show that electric field  $E$  did not exceed  $0.15 \text{ V cm}^{-1}$  in processing chamber owing to collimating effect of the third electromagnet M3 (figure 1). A small value of electric field results in low directed and thermal energies of ions.

Figure 4 shows the spectral profiles of Al 3961 Å line measured parallel and transverse to the flow directions. The Fabry–Perot mirrors spacing is 5 mm in this case, and the instrument broadening is  $0.012 \text{ Å}$ . The first line, measured from end reactor window, is shifted to shorter wavelength due to the macroscopic motion. Its width is larger because the profile obtained is integrated along the direction of observation and includes both the directed and the random energy components [16]. The value of this shift is  $0.01 \text{ Å}$ , which corresponds to the directed velocity and energy of  $760 \text{ m s}^{-1}$  and  $0.08 \text{ eV}$ , respectively. This small shift is not very reliable for estimation. Part of sputtered aluminium atoms fly upstream along the line of observation and produce red shift. The width of the spectral line measured perpendicular to the flow is smaller, and it was used to calculate the transverse temperature of the sputtered aluminium atoms.

For spectral line Al 3961 Å, the excited state lifetime is of the order of  $10^{-8}$  s. Using an upper velocity of  $2 \times 10^4 \text{ m s}^{-1}$  for sputtered aluminium atoms, excited atoms are likely to move less than 0.2 mm before emitting a photon. This distance is small compared to the aperture of the optical measurement system. Thus, it is reasonable to assume that excited sputtered aluminium atoms emit from the same position where they are excited.

The velocity distribution of the sputtered atoms is non-Maxwellian. Sputtered atoms are not well thermalized for several mean free paths. Nevertheless, at pressure above 1 mTorr the experimental contour, measured perpendicular to the flow, is well described by the Voigt function.

Aluminium has a nuclear spin  $I = \frac{5}{2}$  and consequently each line possesses a hyperfine structure. Figure 5 shows the hyperfine structure for the considered Al 3961 Å line. The upper level  $4^2S_{1/2}$  is split into two hyperfine sublevels with a



**Figure 5.** Hyperfine structure of the aluminium 3961 Å line.

separation of  $0.042 \text{ cm}^{-1}$  ( $0.0066 \text{ Å}$ ). The lower level  $3^2P_{3/2}$  is split into four components with a total width of  $0.028 \text{ cm}^{-1}$ . Al 3961 Å line consists of six components according to the selection rule for quantum number  $F$ :  $\Delta F = 0, \pm 1$ . The numbers near the arrows denote the relative intensities of components calculated by intensity rules [17]. The distances between the components of the bottom level are very small, therefore the hyperfine structure can be approximated to two components with spacing  $0.03 \text{ cm}^{-1}$  ( $0.005 \text{ Å}$ ) and relative intensities 120:228. Minimum Gaussian line width of Al 3961 Å line, measured in the experiment, was equal to  $0.023 \text{ Å}$ . Modelling studies show that the error in line width is 7% in this case, if hyperfine splitting is neglected. For such line width hyperfine structure can be ignored.

The Al 3961 Å line is the resonance line and can be affected by self-absorption. The absorption coefficient in the spectral line is given by [12]

$$\int \kappa_L(\lambda) d\lambda = \frac{0.0268 N_i f_{ik} \lambda^2}{c} \quad (1)$$

where  $N_i$  is the atom density at lower level,  $f_{ik}$  is the oscillator strength,  $\lambda$  is the spectral line length and  $c$  is the velocity of light. The absorption coefficient in the centreline  $k_L(\lambda_0)$  can be evaluated as follows:  $k_L(\lambda_0) \approx 0.0268 N_i f_{ik} \lambda^2 / c \Delta\lambda$ , where  $\Delta\lambda$  is spectral line width. The oscillator strength for the Al 3961 Å line is equal to 0.12 [18]. Mean aluminium density for stream diameter  $d = 10 \text{ cm}$  was less than  $2 \times 10^{10} \text{ cm}^{-3}$  at a distance of 17.5 cm from the target for measurement conditions. Then,  $k_L(v)d = 0.01$  for  $\Delta\lambda = 0.03 \text{ Å}$  and the ratio of transmitted to incident intensity is  $\exp(-k_L(\lambda)d) = 0.91$ . There was an increase in the intensity of the Al 3961 Å line with increase of power and pressure, but no plateau on the line profile was observed.

Figure 6 shows the transverse temperature of sputtered aluminium atoms  $T_{\text{Al}}$  as a function of gas pressure in argon

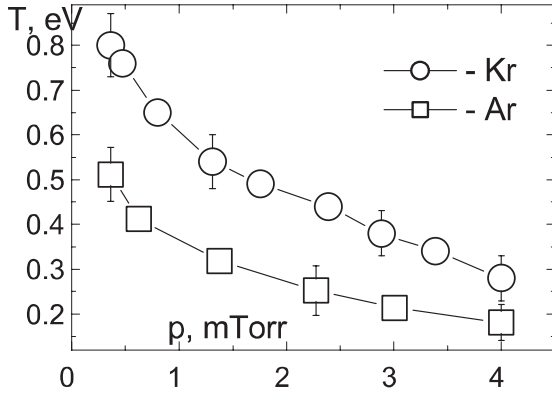


**Figure 6.** The transverse temperature of sputtered aluminium as a function of pressure.  $D = 17.5$  cm,  $W_{\mu} = 600$  W.

and krypton discharges. The temperature decreases from 0.8 to 0.28 eV when krypton pressure rises from 0.4 to 4 mTorr. For discharge in argon, this temperature falls from 0.5 to 0.18 eV for the same condition. The average fraction of energy lost by an aluminium atom in collision with background gas atom is

$$\delta = \frac{2m_{\text{Al}}m_{\text{g}}}{(m_{\text{Al}} + m_{\text{g}})^2}$$

where  $m_{\text{Al}} = 27$  is the mass of the aluminium atom and  $m_{\text{g}} = 40$  (for Ar) and  $m_{\text{g}} = 84$  (for Kr) are the masses of the gas atoms. The value of  $\delta$  is equal to 0.48 for Ar and 0.37 for Kr, which means that an aluminium atom loses greater energy on collision with an argon atom. The sputtered atoms undergo few collisions with background gas atoms at the distance of 17.5 cm. The measured energy is much less than the most probable energy of sputtered atoms leaving the target (1.7 eV), but only partially thermalized.

The energy distribution of the sputtered atom is assumed to obey the Thompson distribution with cosine angular distribution. As shown in [6] with Monte-Carlo simulation, this assumption can be used because the energy of the incident ions is greater than 400 eV. The Thompson distribution for an Al target peaks at 1.7 eV—one-half the surface binding energy, but due to the high-energy tail, the average energy of the sputtered Al atoms is about 9 eV. Using rough approximation of hard-sphere interaction potential, the energy loss of the atom as it passes through the sputtering gas can be estimated from the following equation:

$$\frac{dE}{dz} = -\frac{\delta E}{\lambda} \quad (2)$$

where  $\lambda = 1/n\sigma$  is the mean free path,  $n$  and  $\sigma$  are the gas density and the collision cross section, respectively. The solution of this equation is  $E = E_0 \exp(-\delta z/\lambda)$ , where  $E_0$  is the initial mean energy of a sputtered atom. For an Al atom slowing down from a mean initial energy  $E_0 = 9$  eV in Ar gas at a pressure of 4 mTorr, gas temperature  $T = 350$  K, and taking the value of  $\sigma = 2.8 \times 10^{-15}$  cm<sup>2</sup>, we get  $E = 0.7$  eV and  $T = (\frac{2}{3})E = 0.47$  eV at a distance  $D = 17.5$  cm. This estimation is more than two times the value obtained in experiments. Equation (2) is valid for sputtered atoms, which are much heavier than the filling gas atoms. For this condition, the deflection of the sputtered atoms from their original direction of motion is sufficiently small. For atoms

of comparable masses, the projectile atom may be scattered through a large angle. The real path from the target to the observation region may exceed 17.5 cm. The estimation obtained above gives an upper limit to the energy of sputtered atoms. If we take into account an attractive part in the interaction potential, path-length correction due to collisions and smaller mass of Al atom in comparison to Cu atom, and sputtering in Ar gas, the present values of energy show good agreement with Monte-Carlo simulation results [5, 6] and Ball *et al*'s experimental results [8] at identical PD values.

The deposition Al flux will be composed of Al ions and neutral atoms. The flux of thermalized neutral metal is

$$\Gamma_{\text{m}} = 0.25v_{\text{th}}n_{\text{Al}} = 0.25n_{\text{Al}} \left( \frac{8T_{\text{Al}}}{M_{\text{Al}}} \right)^{1/2} \quad (3)$$

where  $v_{\text{th}}$ ,  $n_{\text{Al}}$ ,  $T_{\text{Al}}$  and  $M_{\text{Al}}$  are the mean thermal velocity, density, temperature and the mass of the metal atom, respectively. Since metal ions are accelerated to the Bohm velocity by the plasma's pre-sheath, the ion flux at the wafer is

$$\Gamma_{\text{Al}^+} = 0.61n_{\text{Al}^+} \left( \frac{T_{\text{e}}}{M_{\text{i}}} \right)^{1/2} \quad (4)$$

where  $n_{\text{Al}^+}$  is the metal ion density. Since  $T_{\text{e}} \gg T_{\text{Al}}$ , the fraction of ionized metal flux  $\Gamma_{\text{Al}^+}/(\Gamma_{\text{Al}^+} + \Gamma_{\text{Al}})$  to a wafer is larger than the fraction of ionized metal in plasma  $n_{\text{Al}^+}/(n_{\text{Al}^+} + n_{\text{Al}})$ . For example, assuming 20% ionization,  $T_{\text{e}} = 3$  eV and  $T_{\text{Al}} = 0.2$  eV, the aluminium ion flux will be 60% in excess of the deposition flux.

## 4. Conclusion

The transverse temperature of sputtered aluminium atoms in ECR krypton and argon plasmas has been measured in the pressure range 0.4–4 mTorr, which is usually used for ECR system operation. The thermalization process is essential to increase the ionization of sputtered metal atoms using the IPVD technique to produce integrated circuit features with high-aspect ratio. At a distance of 15 cm downstream of the target and a pressure of 4 mTorr, this temperature is 0.28 and 0.18 eV in krypton and argon discharges, respectively.

## Acknowledgments

This work was supported by the Ministry of Education of the Russian Federation under grant of the program 'Scientific investigations on priority directions of science and engineering'.

## References

- [1] Nichols C A, Rossnagel S M and Hamaguchi S 1996 *J. Vac. Sci. Technol. B* **14** 3270
- [2] Gorbatkin S M, Poker D B, Roades, Doughty C, Berry L A and Rossnagel S M 1996 *J. Vac. Sci. Technol. B* **14** 1853
- [3] Rauf S and Venztek P L 2001 *J. Appl. Phys.* **89** 2535
- [4] Westwood W D 1978 *J. Vac. Sci. Technol.* **15** 1
- [5] Turner G M, Falconer I S, James B W and McKenzie D R 1989 *J. Appl. Phys.* **65** 3671
- [6] Yamamura Y and Ishida M 1995 *J. Vac. Sci. Technol. A* **13** 101
- [7] Stuart R V, Wehner G K and Anderson G S 1969 *J. Appl. Phys.* **40** 803

- [8] Ball L T, Falconer I S, McKenzie D R and Smelt J M 1986 *J. Appl. Phys.* **59** 720
- [9] Rossnagel S M 1998 *J. Vac. Sci. Technol. B* **16** 3008
- [10] Poluektov N P and Tsar'gorodzev Yu P 1996 *Instrum. Exp. Tech.* **39** 611
- [11] Poluektov N P, Kharchenko V N and Usatov I G 2001 *Plasma Phys. Rep.* **27** 625
- [12] Lochte-Holtgreven W 1968 *Plasma Diagnostics* (Amsterdam: NHPC)
- [13] Nakano T, Sadeghi N and Gottscho R A 1991 *Appl. Phys. Lett.* **58** 458
- [14] Nakano T and Samukama S 1997 *Japan. J. Appl. Phys.* **36** (Pt.1) 4597
- [15] Tsu D V, Young R T, Obninsky S R, Klepper C C and Berry L A 1995 *J. Vac. Sci. Technol. A* **13** 935
- [16] Efremov N P and Poluektov N P 1998 *J. Quant. Spectrosc. Radiat. Transfer* **60** 523
- [17] Frish S E 1963 *Optical Spectrum of Atoms* (Moscow: Fizmatgiz)
- [18] Radzig A A and Smirnov B M 1968 *Atoms and Ions Parameters* (Moscow: Energy)

# Summary of Comments on pss163948

---

## Page: 2

---

Sequence number: 1

Author:

Date: 6/12/03 5:14:57 PM

Type: Note

Au: Please check Figure 2 is of poor quality

Sequence number: 2

Author:

Date: 6/12/03 5:15:05 PM

Type: Highlight

Figure 2.

## Page: 4

---

Sequence number: 1

Author:

Date: 6/12/03 5:16:38 PM

Type: Highlight

Roades,

Sequence number: 2

Author:

Date: 6/12/03 5:17:03 PM

Type: Note

Au: Please provide initials for author name